Ultrasonics Sonochemistry 20 (2013) 338–344

Contents lists available at SciVerse ScienceDirect

Ultrasonics Sonochemistry

journal homepage: www.elsevier.com/locate/ultson

Ultrasonic emulsification of food-grade nanoemulsion formulation and evaluation of its bactericidal activity

Vijayalakshmi Ghosh, Amitava Mukherjee, Natarajan Chandrasekaran *

Centre for Nanobiotechnology, VIT University, Vellore 632014, Tamilnadu, India

ARTICLE INFO

Article history:
Received 14 March 2012
Received in revised form 7 August 2012
Accepted 8 August 2012
Available online 23 August 2012

Keywords:
Basil oil
Ultrasonic emulsification
Nanoemulsion
Antibacterial activity
Estragole
Escherichia coli

ABSTRACT

Basil oil (*Ocimum basilicum*) nanoemulsion was formulated using non-ionic surfactant Tween80 and water by ultrasonic emulsification method. Process of nanoemulsion development was optimized for parameters such as surfactant concentration and emulsification time to achieve minimum droplet diameter with high physical stability. Surfactant concentration was found to have a negative correlation with droplet diameter, whereas emulsification time had a positive correlation with droplet diameter and also with intrinsic stability of the emulsion. Stable basil oil nanoemulsion with droplet diameter 29.3 nm was formulated by ultrasonic emulsification for 15 min. Formulated nanoemulsion was evaluated for antibacterial activity against *Escherichia coli* by kinetics of killing experiment. Fluorescence microscopy and FT-IR results showed that nanoemulsion treatment resulted alteration in permeability and surface features of bacterial cell membrane.

1. Introduction

Nanoemulsions are metastable submicron oil-in-water dispersions with droplet diameter in the range of 10–100 nm [1]. Potential advantages of nanoemulsions over conventional emulsions like high physical stability, high bioavailability and low turbidity make them attractive systems for application in food, cosmetics and pharmaceutical industry. Nanoemulsions serve as delivery agents for lipophilic bioactive compounds such as drug in the pharmaceutical industry [2,3], for flavors [4] and antimicrobial agents [5] in the food industry, for solubilizing water-insoluble pesticides [6] in agrochemical industry and as vehicle for skincare and personal products in cosmetics [7,8].

Ultrasonic emulsification is a high energy method to develop nanoemulsion. This method is documented as fast and efficient technique for formulating stable nanoemulsion with very small droplet diameter and low polydispersity [9]. It utilizes sound waves with frequency more than 20 kHz by using a sonotrode to cause mechanical vibrations followed by the formation of acoustic cavitation. Collapse of these cavities generates powerful shocks waves which breaks the coarse droplets [10]. Size of droplet diameter can be controlled by optimizing the process parameters such as oil concentration, emulsifier concentration, mixing ratio of oil and surfactant, viscosity of continuous phase, emulsification time and energy input [11]. Using megasonic irradiation (frequency in the range of mega Hz) surfactant-free transparent nanoemulsions have been reported which are stable even in the absence of surfactant [12,13].

Basil (*Ocimum basilicum*) is traditionally used as a medicinal plant for the treatment of several diseases including headache, cough and constipation [14]. Basil oil is a source of phenol derivatives such as eugenol, methyl eugenol, estragole, chavicol and linalool [15] etc., which possesses antimicrobial, antioxidant and insecticidal activity [16–18].

Formulation of nanoemulsion by ultrasonic emulsification has been reported by several works. But it was stable for few weeks only [19]. Also, there are not many reports on nanoemulsion with droplet diameter below 50 nm [20,21]. So, the objective of the present work is to optimize process parameters to formulate basil oil nanoemulsion with very small droplet diameter with long kinetic stability. We also have investigated the bactericidal activity of the formulated emulsion along with the mode of action.

2. Materials and methods

2.1. Chemical reagents

Basil oil and Tween80 were obtained from Sigma Aldrich, India. For all the experiments deionised and Milli-Q (Millipore Corporation) water was used.

2.2. GC–MS analysis

Constituents of basil essential oil were analyzed by GC–MS (JEOL GCMATE II). Carrier gas used was helium gas at a flow rate

* Corresponding author. Tel.: +91 416 2202624; fax: +91 416 2243092.
E-mail address: nchandrasekaran@vit.ac.in (N. Chandrasekaran).

1350-4177/$ - see front matter © 2012 Elsevier B.V. All rights reserved.
http://dx.doi.org/10.1016/j.ultsonch.2012.08.010

of 1 ml/min. The samples were injected with a split ratio of 1:10. Injector temperature was 80 °C and detector temperature was 275 °C. Mass spectra was recorded over 40–400 amu range with 70 eV of ionization energy and ion source temperature 240 °C. Identification of components of oil was done by matching the obtained mass spectra data with NIST MS search version on Wiley library.

2.2.1. Nanoemulsion preparation

Nanoemulsion was formulated using basil oil, non-ionic surfactant Tween80 (HLB-15) and water. Tween80 was preferred to be used as surfactant because it has a high hydrophilic and lipophilic balance value, which is equal to 15. Tween80 is non-ionic in nature and stabilizes emulsion droplets by stearic stabilization. Also, being a low molecular weight surfactant it is efficient in minimizing droplet size better than polymeric surfactants. Concentration of basil oil (6% v/v) was fixed for all the emulsion formulations. Coarse emulsion was prepared by mixing oil and surfactant in different ratios (v/v) 1:1, 1:2, 1:3 and 1:4, followed by the addition of water. Then, the coarse emulsion was subjected to ultrasonic emulsification using a 20 kHz Sonicator (Ultrasonics, USA) with a maximum power output of 750 W. Energy input was given through sonotrode containing a piezoelectric crystal with a maximum probe diameter of 13 mm. It generates intensive, disruptive forces to minimize droplet diameter. Sonicator probe was symmetrically dipped into coarse emulsion, and the sonication process was carried out for different emulsification time. The temperature difference between initial coarse emulsions to final nanoemulsion was less than 10 °C. Heat is generated during the prolonged process of emulsification by high energy method like ultrasonic emulsification. This heat is nullified by placing the sample container in a bigger beaker containing ice. Hence the temperature difference was minimized. Then, the formulated nanoemulsion was characterized and also stability of the emulsion was investigated. All the characterization process was done in room temperature.

2.3. Characterization of nanoemulsion

2.3.1. Droplet size distribution and morphology

Measurement of droplet size and polydispersity index (PDI) of nanoemulsion formulations was determined using 90 plus particle size analyser (Brookhaven Instruments Corporation, USA). Droplet size was analysed by dynamic light scattering technique. As the nano size droplets undergo Brownian motion in emulsion formulation, the intensity of scattered light will vary. This intensity fluctuation in scattered light is measured by the dynamic light scattering technique. The droplet radius (R) can be calculated from Stokes-Einstein equation (Eq. (1)) [22]:

$$D = kT/6\eta R \quad (1)$$

where, D is the translational diffusion coefficient, k is the Boltzmann's constant, T is absolute temperature and η is the viscosity of the medium. All the formulations were diluted with milli-Q (Millipore corporation) double distilled water prior to experiment to eliminate the effect of viscosity caused due to ingredients and also to reduce multiple scattering effect.

Visualization of morphology and structure of basil oil nanoemulsion was carried out by transmission electron microscopy (TEM). To perform TEM observations, a drop of emulsion (negatively stained with phosphotungstic acid) was placed on copper grid and was allowed to dry in vacuum for 3 h. Micrographs were acquired by using a transmission electron microscope (Tecnai-10, Philips) with a W-source and operating at 80 kV.

AFM served for the confirmation of droplet size measurements, and also to determine shape and surface morphology of basil oil nanoemulsion. AFM was performed using (Nanosurf Easy Surf 2, Switzerland). Diluted emulsion samples were drop coated onto a glass slide, air dried to remove excess water, and scanning was carried out at the rate of 100 mVs^{-1} in the range of 50 μm × 50 μm.

2.3.2. Physicochemical characterization

Viscosity of the nanoemulsion formulations were measured as such without dilution using a Brook Field Viscometer (model LVF 69726) with a UL-adapter. All the experiments were carried out at 25 °C in triplicate. Measurement of conductivity of the nanoemulsion formulations was performed using CM 180 Conductivity Meter. pH of all the nanoemulsion formulations were checked using a pH meter (model 361, Systronics) at room temperature.

Turbidity analysis of the formulated nanoemulsions was carried out by measuring the absorbance of undiluted samples at 600 nm using a UV–Visible spectrophotometer (UV–Visible Spectrophotometer 2201, Systronics, India).

For zeta potential analysis, all the samples were diluted with deionised water prior to use. Zeta potential measurement was done using a 90 plus particle size analyser (Brookhaven Instruments Corporation, USA).

2.3.3. Stability of emulsion

The emulsion developed by ultrasonic emulsification was subjected to centrifugation at 10,000 rpm for 30 min and the resistance of emulsion to centrifugation was studied.

Intrinsic stability was studied by storing the emulsion at room temperature. It was then observed for any phase separation or creaming. Also, change in droplet diameter was studied at different interval of time.

2.4. Antimicrobial activity

2.4.1. Kinetics of killing

Basil oil nanoemulsion formulation with oil to surfactant (v/v) ratio of 1:3 was preferred for studying antibacterial efficacy due to its lowest droplet diameter. Kinetics of killing experiment was performed by the method described by Al-Adham et. al. [23]. Overnight culture of *Escherichia coli* (NCIM 2809) was centrifuged at 5000*g* for 10 min. It was then washed twice in phosphate buffered saline (PBS, pH 7.4), and test culture with known inoculum size (1×10^8 CFU/ml) was prepared. 1% v/v of this culture was then challenged with undiluted and nanoemulsion formulations. For viable counts, 0.1 ml of the sample was taken from each tube and spread onto nutrient agar plates. Viable colonies were counted after incubation at 37 °C for 24 h.

2.4.2. Live and dead staining using fluorescence microscopy

Fluorescence microscopy was done to visualize the extent of membrane damage of nanoemulsion treated *E. coli* cells. Live and dead discrimination staining experiment was carried out according to the protocol described by Jakopec et al. [24] with minor modifications. Overnight grown culture of *E. coli* was harvested. A known concentration of culture inoculum (10^6 CFU/ml) was treated with 10-fold diluted 1:3 ratio of basil oil nanoemulsion formulation for 30 min. Bacteria pellet was obtained by centrifuging at 5000 rpm for 10 min followed by two times washing in PBS. To 250 ml of bacterial suspension, 2 μl each of acridine orange (15 μg/ml of PBS) and ethidium bromide (50 μg/ml in PBS) were added. After 5 min of incubation, centrifugation was done to remove unbound dyes and the pellet was resuspended in PBS. Images were then captured using a fluorescence microscope (Leica, DM-2500) supported with Leica-DFC-295 camera and Leica-Application Suite 3.8 processor.

2.4.3. Fourier transform infrared spectroscopy (FT-IR)

Structural modifications at the molecular level of *E. coli* upon treatment with basil oil nanoemulsion were analyzed by FT-IR spectroscopy. A known concentration of culture inoculums (1×10^6 CFU/ml) was treated with 1:10 dilution of basil oil nanoemulsion (1:3 ratio). Interaction was continued for a period of 30 min at 30 °C. Then, the cells were washed twice with phosphate buffered saline (pH 7.4). Samples were prepared by mixing required amount of pellet (both treated cells and control cells without nanoemulsion treatment) with potassium bromide crystals and FT-IR spectroscopic analysis was done. The Perkin Elmer Spectrum1 FT-IR instrument was used for FT-IR analysis, which has globar and mercury vapor lamp as sources. It utilizes Scanning was carried out in the range from 450–4000 cm^{-1} with a typical resolution of 1.0 cm^{-1}.

3. Results and discussion

3.1. Basil oil analysis

Qualitative analysis of the as obtained basil oil was done using GC-MS. Fig. 1 shows the chromatograph of basil oil. Estragole was found to be the major component of the oil with 88% of total peak area. There were two minor peaks were also observed corresponding to eugenol (7.8%) and linalool (4.2%).

3.2. Characterization of nanoemulsion

3.2.1. Droplet size distribution

Droplet sizes of the nanoemulsions after 15 min of ultrasonic emulsification are shown in Table 1. Nanoemulsion with 1:1 (v/v) ratio of oil (6% of total emulsion volume) and surfactant (6% of total emulsion volume) respectively exhibited highest droplet diameter (41.15 ± 0.45 nm). Tween80 was used as surfactant as it has a high hydrophilic–lipophilic balance (HLB-15) and favorable for oil-in-water emulsion. Also, being a small molecule surfactant Tween80 is comparatively effective in minimizing droplet diameter than polymers due to their rapid adsorption onto droplet surface [25]. With an increase in surfactant concentration, the mean droplet diameter of the emulsion was found to be decreased. Nanoemulsion with 1:2 (v/v) and 1:3 (v/v) ratio of oil and surfactant showed droplet diameter of 31.65 nm and 29.6 nm respectively. These results go in accordance with the earlier reports that minimum droplet size can be achieved at low oil surfactant ratio [26]. The total free energy required for nanoemulsion formation is positive and thus the process is non-spontaneous. Surfactant aid the process by decreasing the free energy required for the formation of nanoemulsion by lowering interfacial tension at oil/water interface [27]. Oil concentration used in the formulation was very low (6% of total emulsion volume) and water was used as continuous phase. Hence, the process fits into Taylor's prediction (Eq. (2)) that, emulsion radius (r) is directly related with interfacial tension [28]:

$$R \propto \frac{\epsilon}{\eta \dot{\varepsilon}} \tag{2}$$

Where ε is the interfacial tension, η is the continuous phase viscosity and $\dot{\varepsilon}$ is the shear rate.

With further increase in surfactant concentration, there was a negligible reduction in droplet diameter. Hence the formulation was optimized at 1:3 ratio of oil and surfactant. Further characterization and application studies were carried out with basil oil nanoemulsion with 1:3 ratio. Fig. 2 shows the droplet size distribution of basil oil 1:3 (v/v) ratio formulation.

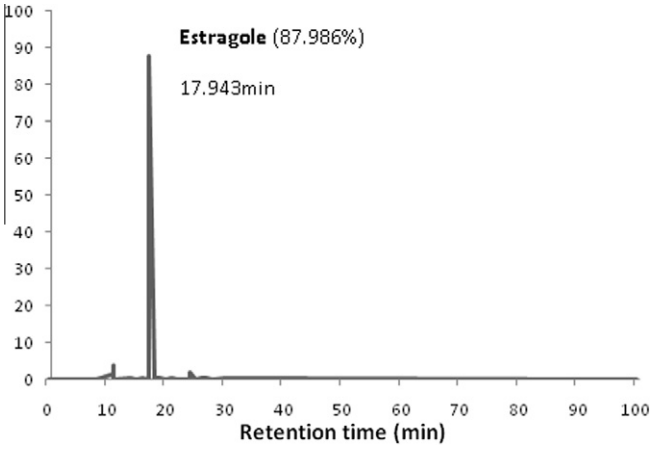

Fig. 1. GC–MS chromatograph of basil oil.

3.2.2. Morphology of emulsion droplets

Morphology of nanoemulsion was visualized by transmission electron microscopy (TEM) and atomic force microscopy (AFM). Fig. 3 shows the TEM image of basil oil nanoemulsion (1:3 ratio). The droplets were spherical in morphology and were in the range of 20–50 nm. The data pertaining to droplet size obtained by TEM analysis correlates with the range of droplet diameter obtained using particle size analyzer (DLS). Nanoemulsion droplets of D-limonene/water emulsion with spherical morphology have already been reported [4].

An AFM micrograph of basil oil nanoemulsion (1:3 ratio) is shown in Fig. 4. Mean droplet diameter was found to be 20.1 nm. It provided additional information for size and shape determination [29]. The morphology of droplets was approximately spherical in shape and smooth surface. Authors have reported AFM image of neem oil nanoemulsion with approximately spherical shape [20].

3.2.3. Effect of surfactant concentration

Physicochemical characterization of all the formulated emulsion was done. Viscosity, turbidity, pH and conductivity of the emulsions are shown in Table 1. Surfactant concentration had a positive correlation with viscosity and a negative correlation on turbidity. Viscosity of the nanoemulsion formulations is 1.77, 2.7, 5.75 and 19.75 cP for 1:1, 1:2, 1:3 and 1:4 (v/v) ratio of basil oil nanoemulsion respectively. As the surfactant concentration increased from 1:1 ratio to 1:4 ratio by maintaining the oil concentration constant, an increasing trend in viscosity of the emulsion was observed (Fig. 5). With elevated surfactant concentration water molecules become trapped in cross-linking chains of surfactants resulting in increased viscosity of the emulsion [30].

Turbidity of the emulsion was expressed in absorbance at 600 nm. There was a sharp decrease in absorbance with the increased surfactant concentration (Fig. 6). This decrease in turbidity was due to minimized droplet diameter at higher surfactant concentration which results in relatively weak scattering making the emulsion system optically transparent [31,32]. Fig. 7 illustrates the visual appearance of the emulsion formulations. Coarse emulsion before subjecting to ultrasonic emulsification comprised of droplets in micro meter range. Hence, it is turbid and milky white in color. After emulsification process is finished, the droplet diameter in the emulsion has reduced to nano meter range. So, change in turbidity of emulsion was observed which further was dependent on surfactant concentration.

3.2.4. Effect of emulsification time on droplet diameter and stability

Emulsification time had a direct correlation with droplet diameter and stability of emulsion. Five minutes of emulsification time resulted in droplet diameter of 57.75, 48.85, 45, and 29.65 nm for 1:1, 1:2, 1:3 and 1:4 (v/v) ratios of oil and surfactant. The emul-

Table 1
Physicochemical characterization of nanoemulsions. All the values are expressed as mean ± SE (n = 3).

Oil:surfactant (v/v)	Mean droplet diameter (nm)	Polydispersity index (PDI)	pH	Conductivity (mS)
1:1	41.15 ± 0.45	0.092 ± 0.001	4.43 ± 0.01	0.08 ± 0.0003
1:2	31.65 ± 0.65	0.236 ± 0.002	4.92 ± 0.01	0.12 ± 0.0006
1:3	29.6 ± 0.2	0.213 ± 0.002	5.53 ± 0.03	0.16 ± 0.0003
1:4	29.3 ± 0.2	0.159 ± 0.002	6.02 ± 0.06	0.17 ± 0.0006

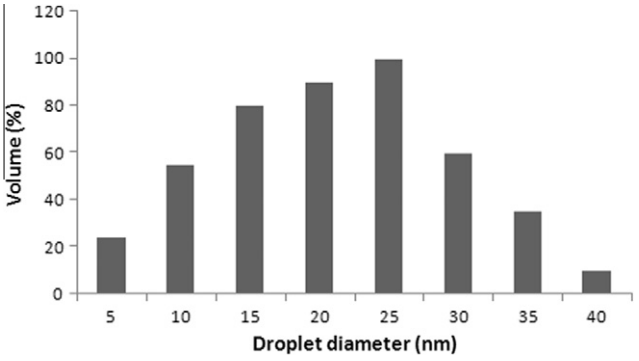

Fig. 2. Droplet size distribution of basil oil nanoemulsion with 1:3 (v/v) ratio of oil and surfactant.

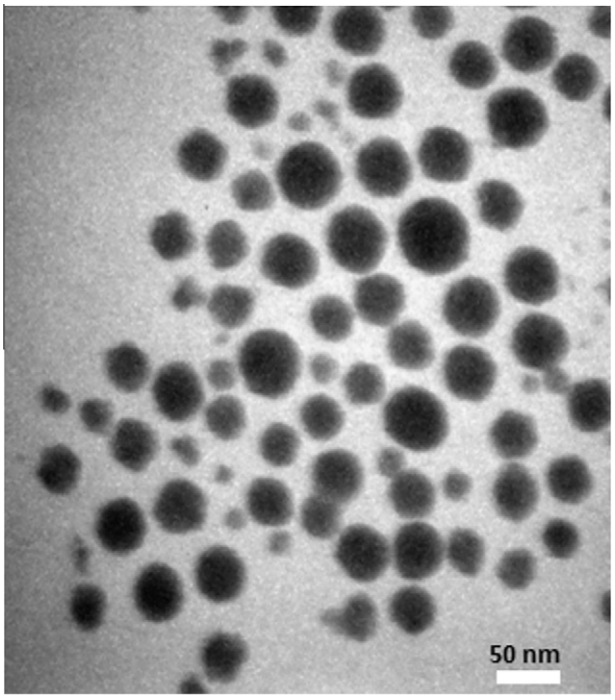

Fig. 3. Transmission electron micrograph of basil oil nanoemulsion with 1:3 (v/v) ratio of oil and surfactant.

sions were stable for 1 month. Phase separation of the emulsions was observed after 1 month of storage. By increasing sonication time to 15 min, reduction in droplet diameter was observed (41.15, 31.65, 29.6 and 29.3 nm for 1:1, 1:2, 1:3, and 1:4 respectively) (Fig. 8). Also, the emulsions were stable after 1 month. No change in droplet diameter was observed and also no phase separation or creaming was observed. Similar trend of decrease in droplet diameter with the increase in emulsification time was observed in case of sunflower oil nanoemulsion formulation [21] [33]. All the formulated emulsions were stable after centrifugation at 10,000 rpm for 30 min.

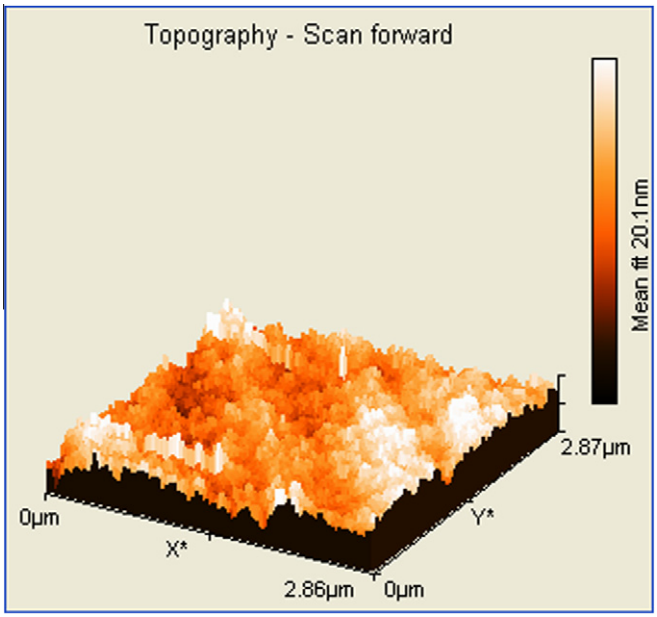

Fig. 4. Atomic force micrograph of basil oil nanoemulsion with 1:3 (v/v) ratio of oil and surfactant.

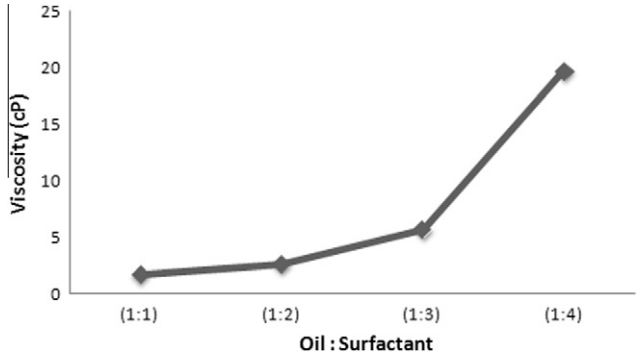

Fig. 5. Effect of surfactant concentration on viscosity of nanoemulsion.

3.2.5. Zeta potential measurements

Zeta potential of the nanoemulsion formulation with 1:3 ratio was found to be −3.70 ± 0.41 mV at emulsion native pH of 5.53. Droplets in the basil oil nanoemulsion were stabilized by non-ionic surfactant. Hence, the absolute magnitude of droplet charge is very low [1,34].

3.3. Antimicrobial activity

3.3.1. Kinetics of killing

Kinetics of killing experiments demonstrated change in viability of *E. coli* upon interaction with basil oil nanoemulsion (1:3 ratio) over a short period of time. After 1 min of interaction with undiluted

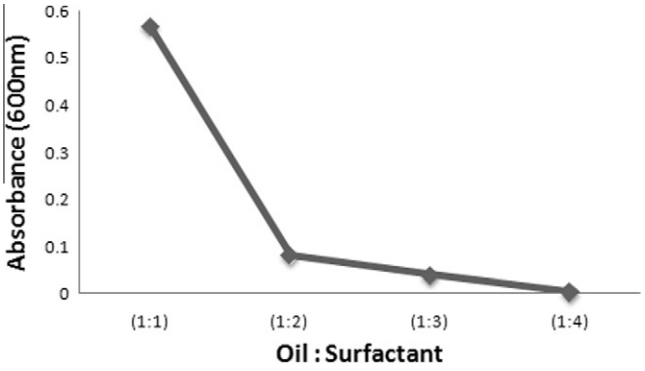

Fig. 6. Effect of surfactant concentration on turbidity of nanoemulsion.

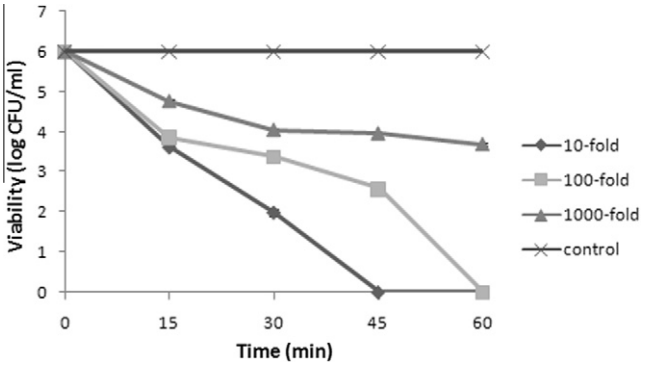

Fig. 9. Time and concentration dependent reduction in viability.

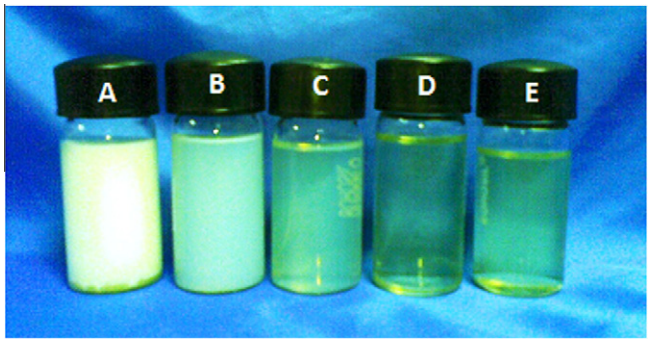

Fig. 7. Visual appearance of emulsion. A - Coarse emulsion before sonication, B - 1:1 (v/v) ratio of basil oil nanoemulsion, C - 1:2 (v/v) ratio of basil oil nanoemulsion, D - 1:3 (v/v) ratio of basil oil nanoemulsion, E - 1:4 (v/v) ratio of basil oil nanoemulsion.

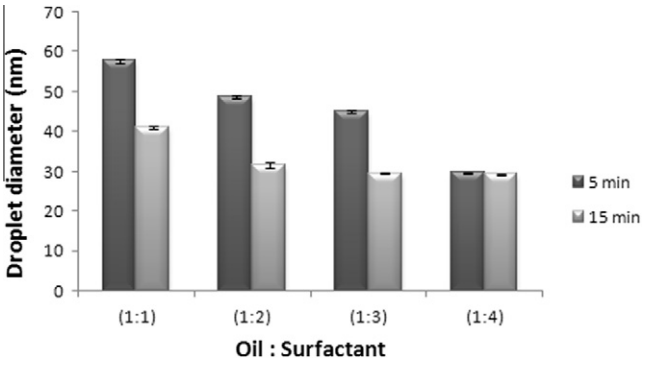

Fig. 8. Effect of sonication time on droplet diameter of emulsion.

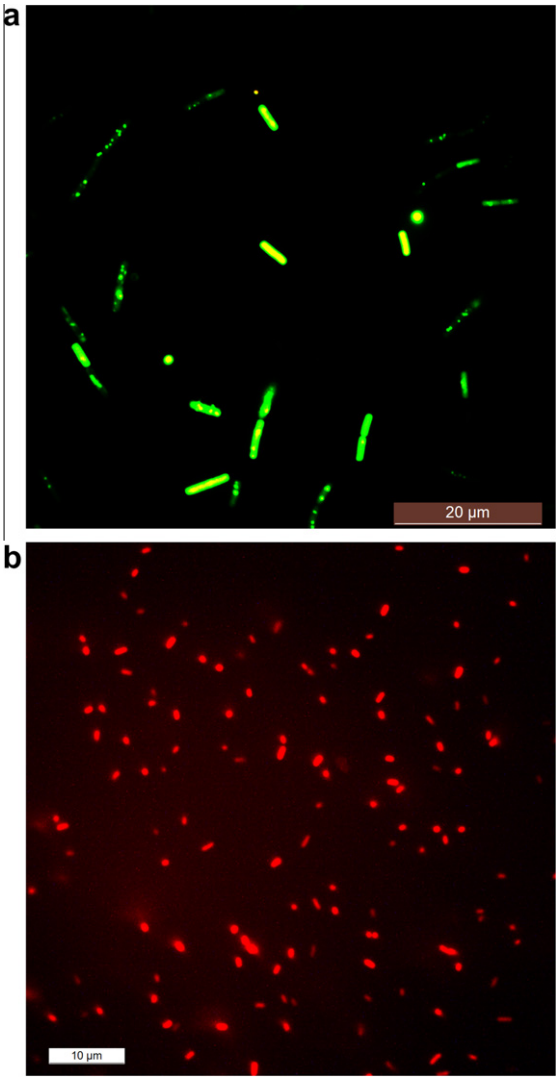

Fig. 10. Fluorescence micrograph of untreated (a) and nanoemulsion treated (b) *E. coli*.

nanoemulsion, no viable cells were obtained. This result is in agreement with the previous reports that, emulsion droplets in the nanometer range are able to cause a 6 log reduction in viable bacteria cells in 1 min [35]. Fig. 9 shows the rate of killing of *E. coli* observed upon treatment with different dilutions of nanoemulsion. More than 60% of viable cells were killed within 15 min of exposure to dilute (10-fold) nanoemulsion. Upon treatment with 10-fold dilution of nanoemulsion, 4 log reduction in viability was observed within 30 min of interaction time and a complete loss of viability was observed in 45 min. Interaction with 100-fold diluted nanoemulsion 50% reduction of viable cells in 45 min and a complete loss of viability in 60 min. Bacteria treatment with 1000-fold diluted basil oil nanoemulsion for 30 min resulted in 2 log reduction in viable cells, and around 40% reduction over a period of 60 min. Bacteria grown in PBS without nanoemulsion treatment is referred as control. All the cells were viable and no cells were killed when they are grown in PBS (control). Unlike nanoemulsions, microemulsions loose bactericidal efficacy upon diluting with water due to significant structural changes in microemulsion droplets [36]. In the present work, nanoemulsion exhibited considerable antibacterial activity even after diluting 10-fold, 100-fold and 1000-fold with water. Antibacterial activity of the nanoemulsion is expected due to the presence of

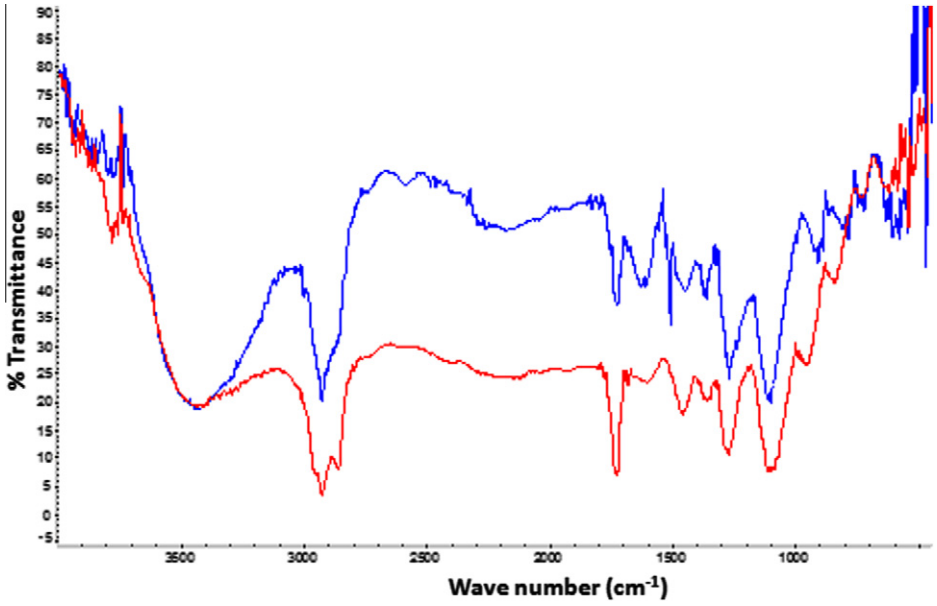

Fig. 11. FT-IR spectra of untreated (--) and nanoemulsion treated (--) *E. coli*.

estragole [37], which is the major component of the essential oil by GC–MS analysis.

3.3.2. Live and dead staining using fluorescence microscopy

Live and dead bacteria cells were visualized by staining with a combination of dyes such as acridine orange and ethidium bromide. Untreated live cells appeared green (Fig. 10a) where as nanoemulsion treated bacteria cells appeared red (Fig. 10b). Acridine orange stains both live and dead bacteria cells, but ethidium bromide stains only those bacteria cells that have lost their membrane integrity. Fluorescence micrograph (Fig. 10b) showed that all the bacteria cells were killed upon treatment with 10-fold diluted basil oil nanoemulsion (1:3 v/v ratio of oil and surfactant) for 30 min. This result supplemented the kinetics of killing results showing complete loss in viability of *E. coli* cells in 30 min of interaction with nanoemulsion.

3.3.3. FT-IR analysis

Fig. 11 shows spectra of *E. coli* cells with (treated) and without (control) interaction with nanoemulsion. Upon treatment with basil oil nanoemulsion, band at 2925 cm^{-1} in untreated cells due to resulting from the asymmetric stretching vibrations of the acyl CH_2 groups in lipid component of cell membrane was shifted to 2927 cm^{-1} in treated cells [38]. Also, change in spectral features was observed in the region between 1800–1300 cm^{-1}. This is attributed to alteration in ester functional groups associated with lipid, protein and nucleic acid. Change in band intensity at 1725 cm^{-1} was observed which is due to alteration in C=O of the ester functional groups of lipids [39]. Spectral changes in the infrared region between 1700–1600 cm^{-1} were observed which indicates that there is significant alteration in protein secondary structure. Change in intensity of the band at 1237 cm^{-1} was observed which is attributed to deformation in bacterial membrane phospholipids [40].

4. Conclusions

A stable food-grade nanoemulsion with droplet diameter 29.6 nm was formulated using basil oil and non-ionic surfactant Tween80 by ultrasonic emulsification which showed antibacterial activity against *E. coli*. In the present study we observed that surfactant concentration, mixing ratio of oil and surfactant, and emulsification time had significant effect on droplet diameter and stability of nanoemulsions. The formulated nanoemulsion showed significant bactericidal activity against *E. coli* even after being diluted. To the best of our knowledge, this is the first report showing basil oil nanoemulsion with very low droplet diameter by ultrasonic emulsification. Formulated nanoemulsions can be further used for food preservation against microbial spoilage.

Acknowledgements

We deeply acknowledge Sophisticated Analytical Instrumentation Facility (SAIF), Department of Science & Technology (DST) at Indian Institute of Technology (IIT), Madras, for GC–MS and FT-IR analysis facility and Tamil Nadu Veterinary College, Chennai, India, for the TEM facility used for this work.

References

[1] D.J. McClements, Edible nanoemulsions: fabrication, properties, and functional performance, Soft Matter 7 (2011) 2297–2316.
[2] M. Kumar, A. Misra, A.K. Babbar, A.K. Mishra, P. Mishra, K. Pathak, Intranasal nanoemulsion based brain targeting drug delivery system of risperidone, Int. J. Pharm. 358 (2008) 285–291.
[3] D. Mou, H. Chen, D. Du, C. Mao, J. Wan, H. Xu, X. Yang, Hydrogel-thickened nanoemulsion system for topical delivery of lipophilic drugs, Int. J. Pharm. 353 (2008) 270–276.
[4] P. Li, B. Chiang, Process optimization and stability of D-limonene-in-water nanoemulsions prepared by ultrasonic emulsification using response surface methodology, Ultrason. Sonochem. 19 (2012) 192–197.
[5] D.J. McClements, E.A. Decker, J.J. Weiss, Emulsion-based delivery systems for lipophilic bioactive components, J. Food Sci. 72 (8) (2007) R109–R124.
[6] L. Wang, X. Li, G. Zhang, J. Dong, J. Eastoe, Oil-in-water nanoemulsions for pesticide formulations, J. Colloid Interface Sci. 314 (2007) 230–235.
[7] O. Sonneville-Aubrun, J.-T. Simonnet, F. L'Alloret, Nanoemulsions: a new vehicle for skincare products, Adv. Colloid Interface Sci. 108–109 (2004) 145–149.
[8] M. Konga, X.G. Chenb, D.K. Kweonc, H.J. Park, Investigations on skin permeation of hyaluronic acid based nanoemulsion as transdermal carrier, Carbohydr. Polym. 86 (2011) 837–843.
[9] C. Lin, L. Chen, Comparison of fuel properties and emission characteristics of two- and three-phase emulsions prepared by ultrasonically vibrating and mechanically homogenizing emulsification methods, Fuel 87 (2008) 2154–2161.
[10] O. Behrend, K. Ax, H. Schubert, Influence of continuous phase viscosity on emulsification by ultrasound, Ultrason. Sonochem. 7 (2000) 77–85.
[11] K. Nakabayashi, F. Amemiya, T. Fuchigami, K. Machida, S. Takeda, K. Tamamitsub, M. Atobe, Highly clear and transparent nanoemulsion

preparation under surfactant-free conditions using tandem acoustic emulsification, Chem. Commun. 47 (2011) 5765–5767.
[12] K. Kamogawa, G. Okudaira, M. Matsumoto, T. Sakai, H. Sakai, M. Abe, Preparation of oleic acid/water emulsions in surfactant-free condition by sequential processing using midsonic megasonic waves, Langmuir 20 (6) (2004) 2043–2047.
[13] S.M. Jafari, E. Assadpoor, Y. He, B. Bhandari, Re-coalescence of emulsion droplets during high-energy emulsification, Food Hydrocolloids 22 (2008) 1191–1202.
[14] S.J. Lee, K. Umano, T. Shibamoto, K.G. Lee, Identification of volatile components in basil (*Ocimum basilicum* L.) and thyme leaves (*Thymus vulgaris* L.) and their antioxidant properties, Food Chem. 91 (2005) 131–137.
[15] I. Almeida, D.S. Alviano, D.P. Vieira, P.B. Alves, A.F. Blank, A.H.C.S. Lopes, C.S. Alviano, M.S. Rosa, Antigiardial activity of *Ocimum basilicum* essential oil, Parasitol. Res. 101 (2007) 443–452.
[16] T. Koga, N. Hirota, K. Takumi, Bactericidal activities of essential oils of basil and sage against a range of bacteria and the effect of these essential oils on *Vibrio parahaemolyticus*, Microbiol. Res. 154 (1999) 267–273.
[17] O. Politeo, M. Jukic, M. Milos, Chemical composition and antioxidant capacity of free volatile aglycones from basil (*Ocimum basilicum* L.) compared with its essential oil, Food Chem. 101 (2007) 379–385.
[18] J.A. Gonzáleza, M. García-Barriusob, M. Gordalizac, F. Amich, Traditional plant-based remedies to control insect vectors of disease in the Arribes del Duero (western Spain): an ethnobotanical study, J. Ethnopharmacol. 138 (2011) 595–601.
[19] P. Li, B. Chiang, Process optimization and stability of D-limonene-in-water nanoemulsions prepared by ultrasonic emulsification using response surface methodology, Ultrason. Sonochem. 19 (2012) 192–197.
[20] C.H. Anjali, Y. Sharma, A. Mukherjee, N. Chandrasekaran, Neem oil (*Azadirachta indica*) nanoemulsion – a potent larvicidal agent against *Culex quinquefasciatus*, Pest Manag. Sci. 68 (2) (2012) 158–163.
[21] T.S.H. Leong, T.J. Wooster, S.E. Kentish, M. Ashokkumar, Minimising oil droplet size using ultrasonic emulsification, Ultrason. Sonochem. 16 (2009) 721–727.
[22] T. Tadros, P. Izquierdo, J. Esquena, C. Solans, Formation and stability of nano-emulsions, Adv. Colloid Interface Sci. 108–109 (2004) 303–318.
[23] I.S.I. Al-Adham, E. Khalil, N.D. Al-Hmoud, M. Kierans, P.J. Collier, Microemulsions are membrane-active, antimicrobial, self-preserving systems, J. Appl. Microbiol. 89 (2000) 32–39.
[24] S. Jakopec, K. Dubravcic, S. Polanc, J. Kosmrlj, M. Osmak, Diazene JK-279 induces apoptosis-like cell death in human cervical carcinoma cells, Toxicol. In Vitro 20 (2) (2006) 217–226.
[25] C. Qian, D.J. McClement, Formation of nanoemulsions stabilized by model food-grade emulsifiers using high-pressure homogenization: Factors affecting particle size, Food Hydrocolloids 25 (2011) 1000–1008.
[26] J.M. Gutiérrez, C. González, A. Maestro, I. Solè, C.M. Pey, J. Nolla, Nano-emulsions: new applications and optimization of their preparation, Curr. Opin. Colloid Interface Sci. 13 (2008) 245–251.
[27] T. Tadros, P. Izquierdo, J. Esquena, C. Solans, Formation and stability of nano-emulsions, Adv. Colloid Interface Sci. 108–109 (2004) 303–318.
[28] G.I. Taylor, The formation of emulsions in definable fields of flow, Proceedings of the Royal Society A146 (1934) 501.
[29] C. Preetza, A. Hauserb, G. Hausec, A. Kramerd, K. Mäder, Application of atomic force microscopy and ultrasonic resonator technology on nanoscale: distinction of nanoemulsions from nanocapsules, Eur. J. Pharm. Sci. 39 (2010) 141–151.
[30] D.I.D.E. Eini, B.W. Barry, C.T. Rhodes, Micellar size, shape and hydration of long-chain polyoxyethylene nonionic surfactants, J. Colloid Interface Sci. 54 (3) (1976) 348–351.
[31] D.J. McClements, Colloidal basis of emulsion color, Curr. Opin. Colloid Interface Sci. 7 (2002) 451–455.
[32] D.J. McClements, Theoretical prediction of emulsion color, Adv. Colloid Interface Sci. 97 (2002) 63–89.
[33] K. Landfester, J. Eisenblätter, R. Rothe, Preparation of polymerizable miniemulsions by ultrasonication, J. Coat. Technol. Res. 1 (1) (2004) 65–68.
[34] S.Y. Tang, S. Manickama, T.K. Wei, B. Nashiru, Formulation development and optimization of a novel Cremophore EL-based nanoemulsion using ultrasound cavitation, Ultrason. Sonochem. 19 (2012) 330–345.
[35] H. Zhang, Y. Shen, P. Weng, G. Zhao, F. Feng, X. Zheng, Antimicrobial activity of a food-grade fully dilutable microemulsion against *Escherichia coli* and *Staphylococcus aureus*, Int. J. Food Microbiol. 135 (2009) 211–215.
[36] P.C. Teixeira, G.M. Leite, R.J. Domingues, J. Silva, P.A. Gibbs, J.P. Ferreira, Antimicrobial effects of a microemulsion and a nanoemulsion on enteric and other pathogens and biofilms, Int. J. Food Microbiol. 118 (2007) 15–19.
[37] K. Carović-Stanko, S. Orlić, O. Politeo, F. Strikić, I. Kolak, M. Milos, Z. Satovic, Composition and antibacterial activities of essential oils of seven *Ocimum* taxa, Food Chem. 119 (2010) 196–201.
[38] A.M. Herrero, P. Carmona, T. Pintado, F. Jiménez-Colmenero, C. Ruíz-Capillas, Olive oil-in-water emulsions stabilized with caseinate: elucidation of protein-lipid interactions by infrared spectroscopy, Food Hydrocolloids 25 (2011) 12–18.
[39] M. Huleihel, V. Pavlov, V. Erukhimovitch, The use of FTIR microscopy for the evaluation of anti-bacterial agents activity, J. Photochem. Photobiol. B 96 (2009) 17–23.
[40] R.R. Dukor, M.N. Liebman, B.L. Johnson, A new, non-destructive method for analysis of clinical samples with FT-IR microspectroscopy, breast cancer tissue as an example, Cell Mol. Biol. 44 (1998) 211–217.